Available online at www.sciencedirect.com
ScienceDirect
Journal of Catalysis 249 (2007) 134–139
JOURNAL OF CATALYSIS
www.elsevier.com/locate/jcat

Role of steps in the reactivity of the anatase $TiO_2(101)$ surface

Xue-Qing Gong *, Annabella Selloni

Department of Chemistry, Princeton University, Princeton, NJ 08544, USA

Received 22 January 2007; revised 4 April 2007

Available online 1 June 2007

Abstract

We studied the adsorption of water, methanol, and formic acid at terraces and steps on the stoichiometric anatase $TiO_2(101)$ surface by means of density functional theory calculations. Our results show that the reactivity of the step edges is distinct from that of the (101) terraces and is instead similar to the reactivity of the extended (112) and (100) surfaces, which are exposed at their facets. More specifically, on the (101) terraces, all molecules are adsorbed in molecular (undissociated) form, and the adsorption energy is rather low (<1 eV). At step D-(112), adsorption energies are significantly larger than on (101) terraces, but molecular adsorption is still favored by water and methanol. At step B-(100), all of the molecules prefer to dissociate, even though the adsorption energy of water is lower than on the (101) terrace. The connection between reactivity and local structure is highlighted, and comparison with available experimental data is provided.

Keywords: Titanium dioxide; Anatase; Density functional theory; Metal oxides; Defect; Surface step; Surface reactivity; Adsorption; Photocatalysis

1. Introduction

Monoatomic height steps are very common defects on metal oxide surfaces and strongly influence their reactivity [1–7]. However, steps on metal oxides have been much less extensively studied than other defects, such as oxygen vacancies, [1,8,9]. Here we consider monoatomic height steps on the (101) surface of the anatase polymorph of titanium dioxide (TiO_2), a very efficient and widely used material for applications in photocatalysis and solar energy conversion [1,10–13]. Among different anatase TiO_2 facets, the (101) surface has the lowest formation energy and is very frequently exposed by anatase nanoparticles [10,14–24]. On this surface, scanning tunneling microscopy (STM) studies have shown the occurrence of trapezoidal islands with monoatomic height step edges along specific directions [25]. Using density functional theory (DFT) calculations, we recently showed that the observed shape and orientation of the islands are determined by two types of step edges—designated D and B—with very low formation energies [26]. In this work, we characterize the reactivities of these steps by performing DFT calculations of their interactions with small "prototype" probe molecules, namely H_2O, CH_3OH, and HCOOH, which are widely used in experiments [27–41]. Because most applications of TiO_2 involve an aqueous environment, the interaction of titania surfaces with water is of special interest. Methanol is a simple prototype for organic compounds and plays an important role in photocatalysis as a hole scavenger [42,43]. HCOOH is a very common organic molecule that, importantly, has the same structure as the anchoring groups of many photosensitizers used for solar energy conversion [44–48]. Therefore, the study of HCOOH adsorption also can provide valuable insight into how photosensitizers connect to TiO_2 surfaces.

2. Calculations

The total energy DFT calculations were carried out within the generalized gradient approximation (GGA) using the PWScf code included in the Quantum-Espresso package [49,50]. Electron–ion interactions were described by ultrasoft pseudopotentials [51], with electrons from C 2s, 2p, O 2s, 2p, and Ti 3d, 4s shells explicitly included in the calculations. Plane-wave basis set cutoffs for the smooth part of the wave functions and the augmented density were 25 and 200 Ry, respectively. The anatase $TiO_2(101)$ surface was modeled as a periodic slab with

* Corresponding author.
E-mail address: xgong@princeton.edu (X.-Q. Gong).

0021-9517/$ – see front matter
doi:10.1016/j.jcat.2007.04.011

6 layers of oxide, with a vacuum between slabs of ∼10 Å. A (2 × 2) surface cell with corresponding 2 × 2 × 1 k-point mesh was used. Steps were modeled using appropriate vicinal surfaces. In particular, we considered the vicinal anatase TiO_2(134) and TiO_2(301) surfaces for steps D and B, respectively [26]. We used a (1 × 2) surface cell together with a 2 × 3 × 1 k-point mesh to study molecular adsorption on the vicinal TiO_2(301) surface. For adsorption on anatase TiO_2(134), we used a (1 × 1) surface cell with corresponding 2 × 3 × 1 k-point mesh. The extended TiO_2(112) and (100) surfaces were modeled using slabs with 4 layers of oxide. A (2 × 1) surface cell with a 2 × 2 × 1 k-point mesh was used to study adsorption on the (100) surface. For the (112) surface, a (2 × 1) surface cell with 2 × 3 × 1 k-point mesh was used. The adsorbate coverage—evaluated with reference to the number of surface Ti_{5c} sites at terraces or step edges—was 0.25 ML on the TiO_2(101), (112), and (100) surfaces and 0.5 ML on the TiO_2(134) and (301) surfaces. To investigate the coverage dependence of adsorption energies, we performed calculations with larger (1 × 2) and (2 × 2) surface supercells for TiO_2(134) and TiO_2(112), respectively (with corresponding 2 × 2 × 1 k-point mesh), and found that changes were very small (<1%).

The molecules were adsorbed on one side of the slab only (hereinafter referred to as the upper surface). During structural optimizations, the adsorbates and all of the atoms of the slab, except those in the bottom surface of anatase TiO_2(101), (100), and (112), were allowed to move (force threshold, 0.05 eV/Å).

3. Results

The optimized structure of the flat anatase TiO_2(101) surface is reported in Fig. 1a. Both fully saturated 3(6)-fold O(Ti) (O_{3c} and Ti_{6c}) atoms and coordinatively unsaturated (cus) 2(5)-fold O(Ti) (O_{2c} and Ti_{5c}) are present on the surface [52]. The displacements of these atoms from their bulk-truncated positions have been described in detail in previous work by our group [23]. Briefly, O_{2c} (O_{3c}) atoms undergo an inward (outward) displacement by ∼0.08 (∼0.2) Å, while Ti_{5c} (Ti_{6c}) atoms are displaced inward (outward) by ∼0.15 (∼0.2) Å. Figs. 1b and 1c show the structures of the two most stable steps, D and B, respectively. Both steps expose Ti_{5c} and O_{2c} atoms, which have the same degree of unsaturation as the cus atoms on the (101) terraces. Step D occurs at the two nonparallel sides of the characteristic trapezoidal islands on the (101) surface and has a TiO_2(112) facet (Fig. 1d), whereas step B is the longer of the two parallel sides of the islands and exposes the low-index anatase TiO_2(100) facet (Fig. 1e) [26]. For better clarity, we call these two steps D-(112) and B-(100), respectively. Further details on the structures and energetics of terraces and steps on the anatase TiO_2(101) surface, including the D-(112) and B-(100) step edges and their corresponding facets, have been given previously [26]. The calculated surface energies are 35.0, 46.3, and 56.3 meV/Å^2 (or 0.56, 0.74, and 0.90 J/m^2) for the extended (101), (100), and (112) surfaces, respectively, whereas the calculated step formation energies are 0.04 eV/Å for the D-(112) step and 0.10 eV/Å for the B-(100) step [26]. It is intriguing that the order of stability of steps B-(100) and D-(112) and that of their corresponding (100) and (112) facets are opposite. This difference may be related in part to the significantly higher density of "D step-like" features on the (112) surface with respect to the density of "B step-like" structures on the (100) surface, which tends to make the (112) surface energetically less favorable.

3.1. Anatase TiO_2(101) terraces

Several theoretical studies of H_2O, CH_3OH, and HCOOH adsorption on the flat anatase TiO_2(101) surface are already available [21,43,44,53]. In agreement with those studies, we find that for all of these three molecules, the most stable ad-

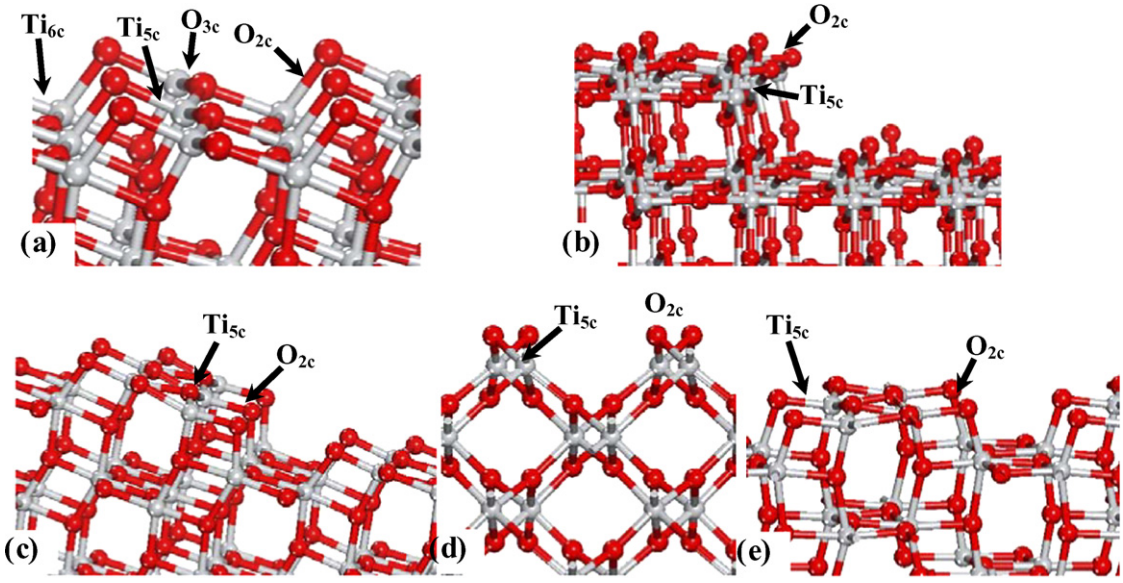

Fig. 1. Calculated structures of (a) anatase TiO_2(101), (b) step D-(112), (c) step B-(100), and the (d) (112) and (e) (100) extended surfaces (side view). The Ti atoms are in gray and O in red. This notation is used throughout this paper.

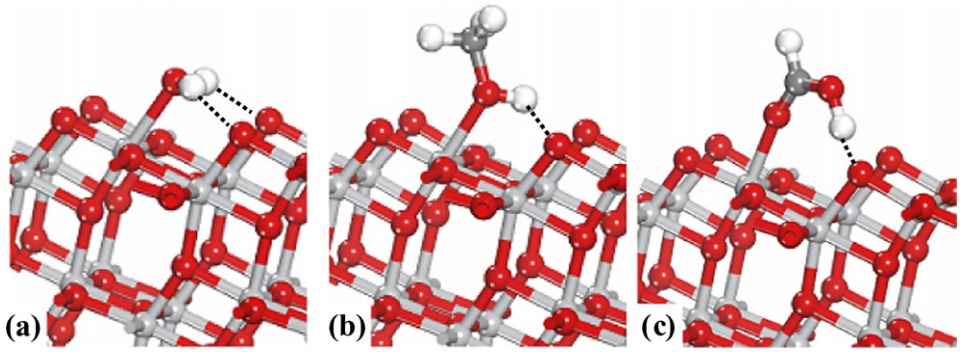

Fig. 2. Calculated structures of molecular (a) H_2O, (b) CH_3OH, and (c) HCOOH adsorbed on anatase TiO_2(101) terraces. C atoms are in deep gray and H in white. The dashed lines indicate H-bonds between molecules and surface O_{2c}.

Table 1
Calculated structural parameters and adsorption energies (E_a) of H_2O, CH_3OH and HCOOH at terraces and steps

Molecule	Surface/step	O–Ti_{5c} (Å)	H–O_{2c} (Å)	E_a (eV)	Figure
H_2O	TiO_2(101)	2.284	2.164	0.78	Fig. 2a
	Step D	2.146	1.638	1.12	Fig. 3a
	TiO_2(112)	2.134	1.569	1.18	Fig. 3b
	Step B	1.817	0.986	0.69(0.65)	Fig. 4a
	TiO_2(100)	1.839	0.986	0.65(0.60)	Fig. 4b
CH_3OH	TiO_2(101)	2.233	2.142	0.73	Fig. 2b
	Step D	2.129	1.677	1.20	Fig. 3c
	TiO_2(112)	2.113	1.604	1.26	Fig. 3d
	Step B	1.793	0.986	0.88(0.70)	Fig. 4c
	TiO_2(100)	1.807	0.986	0.82(0.62)	Fig. 4d
HCOOH	TiO_2(101)	2.118	1.403	1.00	Fig. 2c
	Step D	2.194/2.098	1.014	1.17	Fig. 3e
	TiO_2(112)	2.116/2.037	0.988	1.56	Fig. 3f
	Step B	2.076/2.116	0.986	1.16	Fig. 4e
	TiO_2(100)	2.091/2.127	0.986	1.18	Fig. 4f

O–Ti_{5c} is the distance between the O of the molecule and the surface Ti_{5c} to which it is attached. H–O_{2c} is the length of the H-bond between the H of the molecule and the nearby surface O_{2c} (in the case of dissociative adsorption it is the bond length of the resulting surface hydroxyl). For H_2O and CH_3OH at step B and on TiO_2(100), adsorption energies in parentheses refer to the molecular (less stable) form.

sorption configuration is molecular (undissociated). As shown in Fig. 2, the molecules bind to the surface via an O–Ti_{5c} bond with a cus surface Ti_{5c} atom and one H-bond (two for water) with a nearby surface O_{2c}. Adsorption energies (E_a) are computed from the difference of total energies of the slab + adsorbate system and the noninteracting clean slab and gas-phase molecule. In this way, we obtain $E_a = 0.78$, 0.73, and 1.0 eV for H_2O, CH_3OH, and HCOOH, respectively. The adsorption energies and the key structural parameters of the adsorbed molecules, listed in Table 1, are also in agreement with those reported in previous studies.

3.2. D-(112) steps and extended TiO_2(112) surfaces

The most stable adsorption structures of H_2O, CH_3OH, and HCOOH at step D-(112), and, for comparison, on the extended TiO_2(112) surface are shown in Fig. 3. The corresponding computed adsorption energies and structural parameters are reported in Table 1. For water and methanol, molecular adsorption is always preferred. Several dissociated configurations, with H and OH (CH_3O) moieties occupying neighboring O_{2c} and Ti_{5c} sites, were considered, but none of them remained stable during optimization, because they all converged to molecular (undissociated) configurations. The H_2O (CH_3OH) adsorption energy increases from 0.78 (0.73) eV on the flat (101) surface to 1.12 (1.20) eV at step D-(112); a similar value, 1.18 (1.26) eV, is found on the extended (112) surface. Correspondingly, also the structures of H_2O (CH_3OH) adsorbed at the D-(112) step edge and on the (112) surface are very similar. For example, the bond distances between the water (methanol) oxygen atom and the surface Ti_{5c} to which it binds are 2.146 (2.129) Å at step D-(112) and 2.134 (2.113) Å on the (112) surface. The H-bond between H_2O (CH_3OH) and the O_{2c} on the lower terrace, which is 1.638 (1.677) Å at step D, is only slightly shorter on the (112) surface, 1.569 (1.604) Å. Analogous H-bonds between H_2O (CH_3OH) and O_{2c} on the (101) surface are much longer (∼2.16 Å on average), which may explain why the water (methanol) adsorption energy is lower on the flat (101) surface.

In contrast to water and methanol, HCOOH is more likely to adsorb dissociatively ($E_a = 1.17$ eV) rather than molecularly ($E_a = 1.11$ eV) at step D-(112). As shown in Fig. 3e, HCOOH loses its H to the O_{2c} on the lower terrace, while the HCOO moiety adsorbs at the corner with one O binding to the Ti_{5c} at

the edge and the other O to the Ti_{5c} at the lower terrace, thus forming a bidentate configuration with O–Ti_{5c} bonds of 2.194 and 2.098 Å, respectively. In addition, a H-bond (1.675 Å) is present between the H and HCOO moieties. For HCOOH at the TiO_2(112) surface, dissociation is also favored. As shown in Fig. 3f, the HCOO moiety forms a bidentate structure similar to that at step D-(112). The corresponding adsorption energy of 1.56 eV is about 0.4 eV higher than that at step D-(112). This may be attributed to the fact that on the (112) surface, both oxygens of the HCOO moiety are bonded to very reactive Ti_{5c} at neighboring edges, whereas at step D-(112), one oxygen binds to a Ti_{5c} at a step edge and the other binds to a Ti_{5c} on the terrace.

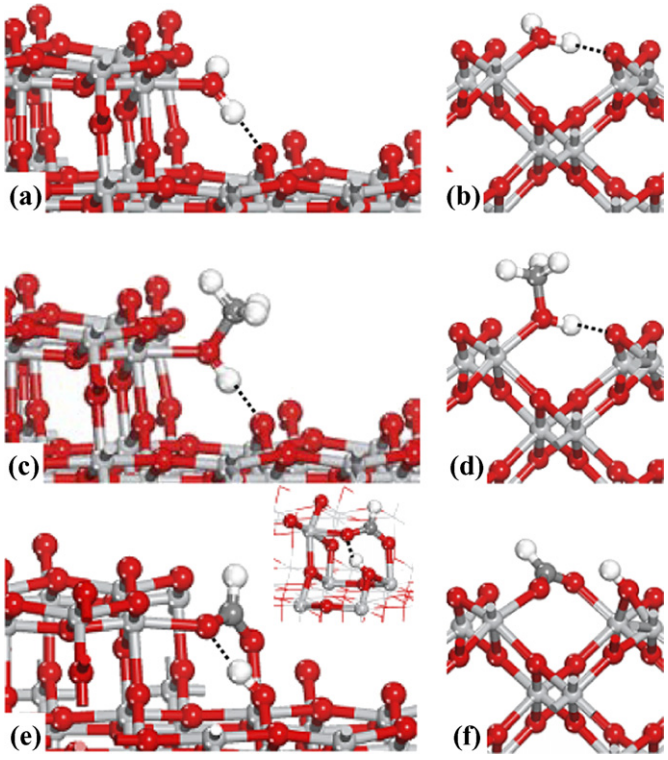

Fig. 3. Calculated structures of (a, b) H_2O, (c, d) CH_3OH and (e, f) HCOOH at step D-(112) (left panel) and on the extended anatase TiO_2(112) (right panel) surfaces. A different side view of the structure is inserted in (e).

3.3. B-(100) steps and extended TiO_2(100) surfaces

Unlike (101) terraces and D-(112) steps, B-(100) steps promote dissociation of all investigated molecules, including H_2O and CH_3OH. In the metastable molecular adsorption configuration, H_2O and CH_3OH bind to the surface via an O–Ti_{5c} bond; on dissociation, they lose one H to a nearby O_{2c} (Fig. 4), and their adsorption energies increase from 0.65 to 0.69 eV for H_2O and from 0.70 to 0.88 eV for CH_3OH (Table 1). This behavior is very similar to that found on the flat (100) surface, where the dissociated (molecular) adsorption energy is 0.65 (0.60) eV for H_2O and 0.82 (0.62) eV for CH_3OH. Preliminary nudged elastic band (NEB) [54,55] calculations using a low number (5) of replicas suggest that H_2O and CH_3OH have relatively low dissociation barriers (∼0.35 eV) on the flat (100) surface, and probably at step B-(100) as well.

For HCOOH, the dissociative chemisorption energy of 1.16 eV is about 0.1 eV higher than the adsorption energy of

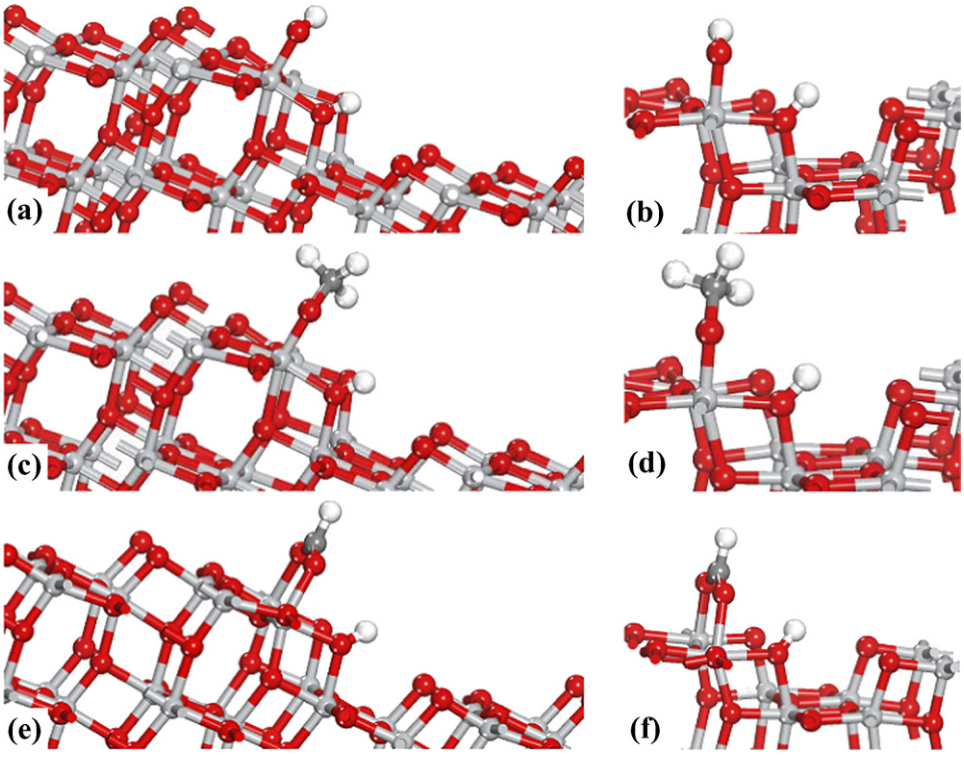

Fig. 4. Calculated structures of (a, b) H_2O, (c, d) CH_3OH and (e, f) HCOOH dissociated at step B-(100) (left panel) and on the extended anatase TiO_2(100) (right panel) surfaces.

the molecular form. Dissociatively adsorbed HCOOH at step B-(100) again takes a bidentate geometry (see Fig. 4e). The two oxygens of the HCOO moiety bind to the two Ti_{5c} atoms at the edge, with O–Ti_{5c} bond lengths of about 2.1 Å, whereas the hydrogen moves to one edge O_{2c}. The structure (see Fig. 4f) and adsorption energy (1.18 eV; see Table 1) of dissociated HCOOH on the (100) surface are very similar to those at the B-(100) step. Incidentally, a similar bidentate geometry for HCOOH adsorption is also found on the anatase TiO_2(001) surface [56]. On the latter surface, however, calculations also yield a metastable monodentate configuration for dissociatively adsorbed HCOOH [56]. In contrast, dissociated monodentate geometries turn out to be unstable for HCOOH at steps B-(100) and D-(112) and on the corresponding anatase TiO_2(100) and (112) surfaces, as they converge to molecular configurations following structural optimization.

4. Discussion

From the foregoing results, it appears that the reactivity of step edges on the anatase TiO_2(101) surface, although distinct from that of (101) terraces, is very similar to the reactivity of the extended surfaces that are exposed at their facets. For H_2O and CH_3OH, D-(112) steps promote stronger adsorption than (101) terraces; however, water and methanol still do not dissociate at step D. In contrast, dissociative adsorption is preferred for water and methanol at step B-(100). Quite interestingly, even after dissociation, H_2O adsorption is energetically less likely at step B-(100) (0.69 eV) than on the (101) terrace (0.78 eV), whereas for CH_3OH, dissociative adsorption at step B-(100) (0.88 eV) is significantly more favorable than adsorption at the (101) terrace (0.73 eV). This suggests that dissociation at step B-(100) should be observed more readily for CH_3OH than for H_2O. This is consistent with recent TPD measurements of water and methanol on anatase (101) [57], which have shown that a small fraction of dissociated molecules is present in the case of methanol, whereas no dissociation occurs for water.

There are noticeable trends in the adsorption energies of H_2O and CH_3OH. At both steps D-(112) and B-(100), the adsorption energy of H_2O is lower than that of CH_3OH (Table 1), even though the two molecules have very similar adsorption configurations (see, e.g., Figs. 3a and 3c). This can be understood by taking into account the relatively higher acidity (weaker RO–H bond strength) of CH_3OH with respect to H_2O [58]. On the flat TiO_2(101) surface, on the other hand, H_2O has a higher adsorption energy than CH_3OH (0.78 vs 0.73; Table 1). This can be explained by the fact that on (101) terraces, H_2O can form *two* H-bonds with O_{2c}, whereas CH_3OH can form only one (see Figs. 2a and 2b), a difference capable of offsetting the stronger O–Ti_{5c} bond formed by methanol with the surface cation (see Table 1, which shows that the O–Ti_{5c} bond distance is shorter for methanol than for H_2O).

For HCOOH, our calculations show that molecular adsorption is favored on (101) terraces, whereas a dissociated bidentate adsorption geometry is favored at both D-(112) and B-(100) step edges. This can be attributed to the fact that the HCOO moiety in a bidentate configuration can form two O–Ti_{5c} bonds with reactive Ti_{5c} atoms at the edges. Thus our results suggest that the binding of HCOOH with stepped anatase TiO_2(101) surfaces is more "robust" than that of H_2O and CH_3OH. This is in agreement with experimental observations for H_2O, CH_3OH, and CH_3COOH competitive adsorption on anatase TiO_2 thin films [27–29]. In addition, our finding of a higher adsorption energy for HCOOH at steps than on terraces is consistent with recent STM measurements indicating that photosensitizer molecules with –COOH anchoring groups are preferentially adsorbed at step edges on rutile TiO_2(110) [59,60].

The strong interaction of HCOOH with step edges suggests that these defect sites also should significantly affect the electronic structure and in turn the efficiency of photosensitizers with COOH anchoring groups. This is supported by calculations of the projected density of states (not shown), which provide indications of a significantly larger overlap between the molecule and surface electronic states at steps than at (101) terraces. Even though HCOOH is too simple to represent a real sensitizer molecule, this result suggests that steps at TiO_2 should significantly facilitate processes like the injection of photoexcited electrons from the sensitizer to the support in solar energy conversion devices based on dye-sensitized TiO_2 materials [61,62].

Acknowledgments

The authors acknowledge the Department of Energy Office of Science for financial support (Grant DE-FG02-05ER15702), and the Pittsburgh Supercomputer Center and Department of Chemistry at Princeton University (Eyring cluster) for computing time. The authors thank U. Diebold for very helpful discussions.

References

[1] U. Diebold, Surf. Sci. Rep. 48 (2003) 53–229.
[2] G. Pacchioni, Surf. Sci. 281 (1993) 207–219.
[3] S.C. Petitto, E.M. Marsh, M.A. Langell, J. Phys. Chem. B 110 (2006) 1309–1318.
[4] M. Baumer, H.J. Freund, Prog. Surf. Sci. 61 (1999) 127–198.
[5] C.C. Chusuei, X. Lai, K. Luo, D.W. Goodman, Top. Catal. 14 (2001) 71–83.
[6] B.K. Min, W.T. Wallace, D.W. Goodman, J. Phys. Chem. B 108 (2004) 14609–14615.
[7] B.K. Min, W.T. Wallace, A.K. Santra, D.W. Goodman, J. Phys. Chem. B 108 (2004) 16339–16343.
[8] O. Bikondoa, C.L. Pang, R. Ithnin, C.A. Muryn, H. Onishi, G. Thornton, Nat. Mater. 5 (2006) 189–192.
[9] H. Iddir, S. Öğüt, N.D. Browning, M.M. Disko, Phys. Rev. B 72 (2005) 081407.
[10] U. Diebold, N. Ruzycki, G.S. Herman, A. Selloni, Catal. Today 85 (2003) 93–100.
[11] A. Hagfeldt, M. Grätzel, Chem. Rev. 95 (1995) 49–68.
[12] A.L. Linsebigler, G.Q. Lu, J.T. Yates Jr., Chem. Rev. 95 (1995) 735–758.
[13] R. Asahi, Y. Taga, W. Mannstadt, A.J. Freeman, Phys. Rev. B 61 (2000) 7459–7465.
[14] V. Shklover, M.K. Nazeeruddin, S.M. Zakeeruddin, C. Barbé, A. Kay, T. Haibach, W. Steurer, R. Hermann, H.U. Nissen, M. Grätzel, Chem. Mater. 9 (1997) 430–439.
[15] H.Z. Zhang, J.F. Banfield, J. Mater. Chem. 8 (1998) 2073–2076.

[16] M.R. Ranade, A. Navrotsky, H.Z. Zhang, J.F. Banfield, S.H. Elder, A. Zaban, P.H. Borse, S.K. Kulkarni, G.S. Doran, H.J. Whitfield, Proc. Natl. Acad. Sci. USA 99 (2002) 6476–6481.
[17] Y. Gao, S.A. Elder, Mater. Lett. 44 (2000) 228–232.
[18] J.R. McCormick, B. Zhao, S.A. Rykov, H. Wang, J.G.G. Chen, J. Phys. Chem. B 108 (2004) 17398–17402.
[19] G.S. Li, L.P. Li, J. Boerio-Goates, B.F. Woodfield, J. Am. Chem. Soc. 127 (2005) 8659–8666.
[20] A.S. Barnard, P. Zapol, Phys. Rev. B 70 (2004) 235403.
[21] A.S. Barnard, P. Zapol, L.A. Curtiss, Surf. Sci. 582 (2005) 173–188.
[22] C. Arrouvel, M. Digne, M. Breysse, H. Toulhoat, P. Raybaud, J. Catal. 222 (2004) 152–166.
[23] M. Lazzeri, A. Vittadini, A. Selloni, Phys. Rev. B 6315 (2001) 155409.
[24] T. Ohno, K. Sarukawa, M. Matsumura, New J. Chem. 26 (2002) 1167–1170.
[25] W. Hebenstreit, N. Ruzycki, G.S. Herman, Y. Gao, U. Diebold, Phys. Rev. B 62 (2000) R16334–R16336.
[26] X.Q. Gong, A. Selloni, M. Batzill, U. Diebold, Nat. Mater. 5 (2006) 665–670.
[27] C.Y. Wang, H. Groenzin, M.J. Shultz, J. Am. Chem. Soc. 126 (2004) 8094–8095.
[28] C.Y. Wang, H. Groenzin, M.J. Shultz, J. Phys. Chem. B 108 (2004) 265–272.
[29] C.Y. Wang, H. Groenzin, M.J. Shultz, J. Am. Chem. Soc. 127 (2005) 9736–9744.
[30] A. Sasahara, H. Uetsuka, H. Onishi, Surf. Sci. 481 (2001) L437–L442.
[31] D.I. Sayago, M. Polcik, R. Lindsay, R.L. Toomes, J.T. Hoeft, M. Kittel, D.P. Woodruff, J. Phys. Chem. B 108 (2004) 14316–14323.
[32] B.E. Hayden, A. King, M.A. Newton, J. Phys. Chem. B 103 (1999) 203–208.
[33] K. Fukui, H. Onishi, Y. Iwasawa, Chem. Phys. Lett. 280 (1997) 296–301.
[34] H. Onishi, Y. Iwasawa, Chem. Phys. Lett. 226 (1994) 111–114.
[35] Y. Morikawa, I. Takahashi, M. Aizawa, Y. Namai, T. Sasaki, Y. Iwasawa, J. Phys. Chem. B 108 (2004) 14446–14451.
[36] A. Gutiérrez-Sosa, P. Martínez-Escolano, H. Raza, R. Lindsay, P.L. Wincott, G. Thornton, Surf. Sci. 471 (2001) 163–169.
[37] R.E. Tanner, A. Sasahara, Y. Liang, E.I. Altman, H. Onishi, J. Phys. Chem. B 106 (2002) 8211–8222.
[38] G.Y. Popova, T.V. Andrushkevich, Y.A. Chesalov, E.S. Stoyanov, Kinet. Catal. 41 (2000) 805–811.
[39] G. Munuera, F. Gonzalez, F. Moreno, J.A. Prieto, in: J.W. Hightower (Ed.), Catalysis: Proeedings of the 5th Interational Congress on Catalysis, North-Holland, Amsterdam, 1973, p. 1159.
[40] K.S. Kim, M.A. Barteau, Langmuir 4 (1988) 945–953.
[41] H. Idriss, V.S. Lusvardi, M.A. Barteau, Surf. Sci. 348 (1996) 39–48.
[42] V.N.H. Nguyen, R. Amal, D. Beydoun, Chem. Eng. Sci. 58 (2003) 4429–4439.
[43] A. Tilocca, A. Selloni, J. Phys. Chem. B 108 (2004) 19314–19319.
[44] A. Vittadini, A. Selloni, F.P. Rotzinger, M. Grätzel, J. Phys. Chem. B 104 (2000) 1300–1306.
[45] B. O'regan, M. Grätzel, Nature 353 (1991) 737–740.
[46] M.K. Nazeeruddin, R. Humphry-Baker, P. Liska, M. Grätzel, J. Phys. Chem. B 107 (2003) 8981–8987.
[47] S. Ushiroda, N. Ruzycki, Y. Lu, M.T. Spitler, B.A. Parkinson, J. Am. Chem. Soc. 127 (2005) 5158–5168.
[48] A.G. Thomas, W.R. Flavell, C. Chatwin, S. Rayner, D. Tsoutsou, A.R. Kumarasinghe, D. Brete, T.K. Johal, S. Patel, J. Purton, Surf. Sci. 592 (2005) 159–168.
[49] J.P. Perdew, K. Burke, M. Ernzerhof, Phys. Rev. Lett. 77 (1996) 3865–3868.
[50] S. Baroni, S. De Gironcoli, A. Dal Corso, P. Giannozzi, Quantum-Espresso, http://www.democritos.it.
[51] D. Vanderbilt, Phys. Rev. B 41 (1990) 7892–7895.
[52] X.Q. Gong, R. Raval, P. Hu, Phys. Rev. Lett. 93 (2004) 106104.
[53] A. Vittadini, A. Selloni, F.P. Rotzinger, M. Grätzel, Phys. Rev. Lett. 81 (1998) 2954–2957.
[54] G. Henkelman, H. Jónsson, J. Chem. Phys. 113 (2000) 9978–9985.
[55] G. Henkelman, B.P. Uberuaga, H. Jónsson, J. Chem. Phys. 113 (2000) 9901–9904.
[56] X.Q. Gong, A. Selloni, A. Vittadini, J. Phys. Chem. B 110 (2006) 2804–2811.
[57] G.S. Herman, Z. Dohnálek, N. Ruzycki, U. Diebold, J. Phys. Chem. B 107 (2003) 2788–2795.
[58] S.J. Blanksby, G.B. Ellison, Acc. Chem. Res. 36 (2003) 255–263.
[59] S. Suzuki, Y. Yamaguchi, H. Onishi, K. Fukui, T. Sasaki, Y. Iwasawa, Catal. Lett. 50 (1998) 117–123.
[60] A. Sasahara, C.L. Pang, H. Onishi, J. Phys. Chem. B 110 (2006) 4751–4755.
[61] S.G. Abuabara, L.G.C. Rego, V.S. Batista, J. Am. Chem. Soc. 127 (2005) 18234–18242.
[62] N.A. Anderson, T.Q. Lian, Annu. Rev. Phys. Chem. 56 (2005) 491–519.